Zebrafish as a Model for Monocarboxyl Transporter 8-Deficiency*

Gad David Vatine[‡§], **David Zada**[‡§], **Tali Lerer-Goldshtein**[‡§], **Adi Tovin**[‡§], **Guy Malkinson**[¶], **Karina Yaniv**[¶], and **Lior Appelbaum**[‡§1]

From the [‡]Mina & Everard Goodman Faculty of Life Sciences and the [§]Leslie and Susan Gonda Multidisciplinary Brain Research Center, Bar-Ilan University, Ramat-Gan 52900 and the [¶]Department of Biological Regulation, The Weizmann Institute of Science, Rehovot 76100, Israel

Background: Mutations in the thyroid hormone transporter MCT8 are associated with the psychomotor retardation Allan-Herndon-Dudley syndrome (AHDS).
Results: In zebrafish, as in humans, mct8 is expressed primarily in the nervous system. Elimination of MCT8 causes severe neural impairment.
Conclusion: MCT8 is a crucial regulator during zebrafish embryonic development.
Significance: Establishment of the first vertebrate model for MCT8 deficiency, which exhibits a neurological phenotype.

Allan-Herndon-Dudley syndrome (AHDS) is a severe psychomotor retardation characterized by neurological impairment and abnormal thyroid hormone (TH) levels. Mutations in the TH transporter, monocarboxylate transporter 8 (MCT8), are associated with AHDS. MCT8 knock-out mice exhibit impaired TH levels; however, they lack neurological defects. Here, the zebrafish mct8 gene and promoter were isolated, and mct8 promoter-driven transgenic lines were used to show that, similar to humans, mct8 is primarily expressed in the nervous and vascular systems. Morpholino-based knockdown and rescue experiments revealed that MCT8 is strictly required for neural development in the brain and spinal cord. This study shows that MCT8 is a crucial regulator during embryonic development and establishes the first vertebrate model for MCT8 deficiency that exhibits a neurological phenotype.

In all vertebrates, thyroid hormones (THs)[2] are essential regulators of development, neurogenesis, growth, and metabolism (1). TH actions are mediated via intracellular activation and inactivation of iodothyronine deiodinases and binding of triio-dothyronine (T_3) to nuclear TH receptors, which regulate gene transcription (1). Thus, to function, THs require efficient transport across the cell membrane. In the last two decades, several transmembrane transporters, which are required for the cellular uptake and efflux of THs, have been functionally described, including the T_3-specific monocarboxylate transporter 8 (MCT8) (2), the T-type amino acid transporter MCT10 (3, 4), and the organic anion-transporting polypeptide 1C1 (OATP1C1) (5), among others (6). Importantly, mutations in MCT8 were associated with the X-linked Allan-Herndon-Dudley syndrome (AHDS), which is characterized by elevated serum T_3 levels and severe psychomotor retardation (7, 8). The mechanism underlying this disorder is thought to involve a defect in the MCT8-dependent neuronal entry of T_3, leading to impaired neurological development. However, little is known about the role of MCT8 in regulating embryonic development and AHDS.

The abnormal serum TH levels observed in AHDS patients were closely replicated in MCT8-deficient mice; however, these mice did not display apparent neurological or behavioral phenotypes (9, 10). Biochemical studies suggested that the transport of T_3, but not its precursor, thyroxine (T_4), is impeded in MCT8-deficient mice, thus additional TH transporters, such as OATP1C1 and MCT10, might compensate for MCT8 deficiency in rodents (11, 12). Clearly, the establishment of additional MCT8-deficient vertebrate models that mimic the pathophysiological condition of AHDS patients is required to complement the mouse model and to better understand the role of MCT8.

The zebrafish is a simple vertebrate model with conserved organization of the central nervous system (CNS), which is ideally suited to study genetics, transcriptional regulation, neuronal development, synaptogenesis, and behavior in live animals (13–15). The larval optical translucency provides the unique ability to visualize single neurons in live animals (13). Importantly, the zebrafish thyroid system, including the hypothalamus-pituitary-thyroid gland axis (16, 17), and the main genes involved in TH signaling (18–21), are largely conserved

between zebrafish and mammals. Moreover, studies on cell lines have recently demonstrated that the zebrafish MCT8 is able to transport THs (22).

In this study, we isolated the complete *mct8* gene and promoter and described the expression pattern of zebrafish *mct8* during development. *mct8* is mainly expressed in the nervous and vascular systems. Using knockdown experiments and *in vivo* imaging, we showed that the lack of MCT8 causes developmental and neurological impairment. These results establish the zebrafish as a model for studying the role of MCT8 and the mechanisms underlying AHDS.

EXPERIMENTAL PROCEDURES

Zebrafish Husbandry—Adult zebrafish were raised and maintained in fully automated zebrafish housing systems (Aquazone, Israel; temperature 28 ± 0.5 °C, pH 7.0, conductivity 300 μS) under 14-h light/10-h dark cycling, and fed twice a day. Embryos were generated by natural spawning and raised in egg water in a 28 ± 0.5 °C, light-controlled incubator, as previously described (23). All animal protocols were reviewed and approved by the Bar-Ilan University Bioethics Committee.

Isolation of mct8 mRNA and Rapid Amplification of cDNA Ends (RACE)—The mouse MCT8 sequence (NM_009197.2) was used as a query in the BLAT algorithm of the University of California Santa Cruz zebrafish genome browser using the Zv9/danRer7 version (genome.ucsc.edu). The partially predicted *mct8* 545-bp sequence that was found on chromosome 14 was used for designing gene-specific primers (GSPs). 5′ and 3′ sequences of the zebrafish *mct8* mRNA were determined using the 5′ and 3′ systems for RACE, according to the manufacturer's protocol (Invitrogen). The specific primers 5′GSP1 (5′-ggaatcatcatggacatcac-3′) 5′GSP2 (5′-tcttgactccaggtatgaggtctcc-3′) and 5′GSP3 (5′-agacgaagctccgatgcacaccagc-3′) were used for the 5′ RACE analysis and the specific primers 3′GSP1 (5′-tgtgatgtttttcgtgcctc-3′) and 3′GSP2 (5′-ccgacgatcccagcatggac-3′) were used for 3′ RACE analysis.

DNA Constructs and Isolation of mct8 Promoter—To prepare probes for whole mount *in situ* hybridization (ISH) experiments, the full coding sequences of the following genes were amplified: *monocarboxylate transporter 8* (*mct8*, JQ966311), *monocarboxylate transporter 10* (*mct10*, NM_001080028), *organic anion transporting polypeptide 1c1* (*oatp1c1*, NM_001044997.3) (19), *type 1 iodothyronine deiodinase* (*dio1*, NM_001007283.1), *type 2 iodothyronine deiodinase* (*dio2*, NM_212789.3) (21), *type 3 iodothyronine deiodinase* (*dio3*, NM_001177935.2) (18), and *myoblast determination protein 1 homolog* (*myod*) (NM_131262) (24). All PCR products were cloned into a pCRII-TOPO vector (Invitrogen) and served as a template to transcribe digoxigenin-labeled antisense mRNA probes.

To isolate the *mct8* promoter, a fragment containing 1,728 bp of genomic 5′ flanking region and 272 bp 5′ UTR of the *mct8* gene was amplified (JQ966310) from zebrafish genomic DNA using the specific primers mct8Pro(2000)F, incorporating a SalI restriction site (5′-cgcctcgaggacaccaacaccccccataatgggac-3′) and mct8UtrR, containing a BglII restriction site (5′-cgcagatctcctacagggagaggatgcagacgcg-3′). The PCR product was double-digested with SalI and BglII, and ligated into a BamHI/

SalI-digested *pT2*-ALR150G (25) upstream of the enhanced green fluorescent protein (EGFP) reporter gene to create the *pT2-mct8:EGFP* construct (Fig. 2*B*). This construct was later used for the preparation of the *Tg(mct8:EGFP)* transgenic line (see below). The GAL4-VP16 transcriptional activator was amplified and subcloned into a NcoI/BglII-digested *pT2-mct8:EGFP*, replacing the EGFP, to create the *pT2-mct8:GAL4* construct. This construct was used to generate the *Tg(mct8:GAL4)* transgenic line (see below).

To prepare *mct8* mRNA *in vitro*, the *mct8* CDS was PCR-amplified by the specific primers BamHIMct8CDSF, containing a BamHI restriction site (5′-cgcggatccatgcactcggaaagcgatgacaac-3′) and SpeIMct8CDSR, containing an SpeI restriction site (5′-cgcactagttcatatgtgtgtctccatgtccgtg-3′). The PCR product was double-digested with BamHI and SpeI, and ligated into a BamHI/SpeI-digested pCS-TP vector (26). The pCS-*mct8*(CDS) construct was linearized by NotI, and mRNA was synthesized *in vitro* using mMESSAGE mMACHINE SP6 Kit (Ambion Inc., Austin, TX).

Whole Mount in Situ Hybridization and Immunohistochemistry Assays—In both whole mount ISH and immunofluorescence experiments, embryos and larvae were fixed in 4% paraformaldehyde overnight at 4 °C, washed in PBS, and stored in 100% methanol. The location and level of mRNA expression were detected by whole mount ISH, as described (27, 28). Digoxigenin-labeled full-length antisense riboprobes for *mct8, mct10, oatp1c1, dio1, dio2, dio3*, and *myod* were transcribed *in vitro* using the vector templates described above, and standard reagents followed the manufacturer's instructions (Roche Applied Science).

In immunofluorescence assays, the larvae were rehydrated with reduced methanol concentration and were incubated in 10 μl/ml of proteinase K for 20 min. The larvae were then blocked with 20% normal goat serum diluted in phosphate-buffered saline (PBS) for 1 h at room temperature. After blocking, larvae were incubated in primary antibodies: rabbit anti-EGFP (SC-8334, Santa Cruz Biotechnology, Santa Cruz, CA), 1:250 dilution; mouse anti-HuC/HuD (A21271, Invitrogen), 1:100 dilution; or mouse anti-GFAP (zrf-1, Zebrafish International Resource Center, Eugene, OR), 1:500 dilution, in blocking buffer overnight at 4 °C. Next, larvae were washed in PBS with Tween and blocked for 1 h. Anti-GFP antibodies were detected with a secondary goat anti-rabbit Alexa Fluor 488 IgG (H+L) antibody (2 mg/ml, A-11034, Invitrogen). Anti-HuC/HuD and anti-GFAP antibodies were detected with a secondary Alexa Fluor 594 goat anti-mouse IgG (2 mg/ml, A-11005, Invitrogen).

Establishment of Stable Transgenic Lines and Colocalization Experiments—To transiently express *pT2-mct8:EGFP* and *pT2-mct8:GAL4/uas:EGFP* in live fish, the constructs were diluted to a concentration of 50 ng/μl and microinjected, using a micromanipulator and a PV830 Pneumatic Pico Pump (World Precision Instruments, Sarasota, FL), into one-cell stage eggs. The embryos were kept in Petri dishes, and the pattern of EGFP expression was monitored throughout their development. To generate *Tg(mct8:EGFP)* and *Tg(mct8:GAL4)* stable transgenic fish, the *Tol2* system was used (25). Capped RNA encoding the *Tol2* transposase and the *pT2-mct8:EGFP* or *pT2-mct8:GAL4* constructs were co-injected independently (in a

concentration of 25 ng/μl each) into fertilized eggs at one-cell stage. The injected fish (generation F0) were raised to adulthood and screened for integration of the transgene into the germline. F0 fish, injected with *pT2-mct8:EGFP*, were crossed with wild-type fish, and F0 fish, injected with *pT2-mct8:GAL4*, were crossed with a *Tg(uas:EGFP)* transgenic line. Transgenic EGFP-positive lines (F1) were screened and isolated using a fluorescent stereomicroscope (M167FC, Leica, Wetzlar, Germany). Four *Tg(mct8:EGFP)* and three *Tg(mct8:GAL4/uas: EGFP)* transgenic lines were obtained. To obtain the *Tg(mct8: GAL4)* line, *Tg(mct8:GAL4/uas:EGFP)* fish were out-crossed with wild-type fish. All lines showed similar patterns of EGFP expression mainly in the central nervous system and along the spinal cord. The transgenic lines that showed the strongest EGFP expression were used in this study. Transgenic fish were established in the nacre$^{-/-}$ mutant (29) background to avoid pigmentation. *Tg(mct8:EGFP/fli:DsRED)* double transgenic larvae were produced by crossing adult *Tg(mct8:EGFP)* and *Tg(fli:DsRED)* (30).

Morpholino Design, Preparation, and Injection—Gene knockdown experiments were performed using the following morpholino-modified antisense oligonucleotides (MO, Gene Tools, Philomath, OR): Gene Tools standard control MO (5′-ctcttacctcagttacaatttata-3′), *mct8*(E2I2)MO (5′-ataaaatcatg-tatttacgtggcga-3′), and *mct8*(UTR)MO (5′-tcctacagggagaggat-gcagacgc-3′). The *mct8*(UTR)MO was designed to block MCT8 translation. To validate the efficiency of the *mct8*(UTR)MO, it was injected into *Tg(mct8:EGFP)* embryos. Because the 5′UTR of *mct8* is present in the *mct8:EGFP* transgene, EGFP expression was eliminated in all injected embryos ($n = 304$, Fig. 5, *F–H*). The *mct8*(E2I2)MO was designed to interfere with the splicing of the second exon/intron and, thereby, to introduce a premature stop codon. Indeed, *mct8* CDS and a 341-bp fragment incorporating parts of the second and third exons (*mct8* E2E3) were PCR-amplified from the cDNA of control MO-injected embryos but not from *mct8*(E2I2)MO-injected embryos (Fig. 4*A*). In all experiments, *Tg(mct8:EGFP)*, *Tg(mct8:GAL4/ uas:EGFP)*, or wild-type embryos were injected with 0.3–1.6 pmol of MO. In rescue experiments, 80 pg of *in vitro* transcribed *mct8* mRNA was co-injected in combination with 1 pmol of *mct8*(E2I2)MO or 0.3 pmol of *mct8*(UTR)MO. Injected embryos were monitored under a M167FC stereomicroscope (Leica, Wetzlar, Germany) and sorted into three groups: normal development, mildly altered development, and severely altered development. Following sorting, embryos were counted, and statistical significances between the different groups were determined by χ-square tests.

Real-time PCR Quantification Assays—The levels of mRNA expression of *dio1*, *dio2*, *dio3*, *tshb*, and *β-actin* were determined using quantitative real-time PCR assays. In three independent experiments, mRNA of 48 h post-fertilization (hpf) larvae injected with 0.5 pmol of *mct8* (UTR) MO, *mct8* (E2I2) MO, or standard control MO were extracted using the RNeasy Protect mini kit according to the manufacturer's instructions (Qiagen). A similar amount of mRNA (280 ng) was reverse transcribed, as described above. Transcript levels were determined by the 7900HT Fast Real-Time PCR System (Applied Biosystems, Foster City, CA) using the KAPA SYBR® FAST qPCR Kit

(Kapa Biosystems, Cambridge, MA) according to the manufacturer's instructions. Triplicate first-strand cDNA aliquots from each sample served as templates in real-time PCR. The relative quantification of *dio1*, *dio2*, *dio3*, and *tshβ* mRNA expression levels were normalized against *β-actin* mRNA expression levels and subjected to the $\Delta\Delta C_T$ method (23). Statistical significance was determined using one-way analysis of variance.

Imaging—An epifluorescence stereomicroscope (Leica M167FC) was used to visualize larvae expressing fluorescent reporters and for imaging whole mount ISH-stained larvae. Pictures were taken using Leica Application Suite imaging software version 3.7 (Leica, Wetzlar, Germany). For confocal imaging, embryos and larvae were anesthetized with Tricaine (0.01%) and placed in low-melting point-agarose (0.5–1.0%) on a specially designed dish filled with embryo water. Similar mounting protocol was used to image fixed embryos subjected to immunohistochemistry. Confocal imaging was performed using either a Zeiss LSM710 or LSM780 upright confocal microscope (Zeiss, Oberkochen, Germany). All images were processed using ImageJ (National Institutes of Health, Bethesda, MD) and Adobe Photoshop (San Jose, CA) software.

Bioinformatical Analyses—The prediction of transcription factor-binding elements, within orthologous putative *mct8* promoters, was performed using the MatInspector software tool (Genomatix, Munich, Germany). Sequences of 2000 bp of 5′ flanking regions upstream to the putative translation start sites from the human, rat, mouse, and zebrafish genomes, were used. Predicted transcription factors found in all four putative promoter sequences, and with the lowest *p* value scores, were selected. The prediction of putative transmembrane domains (TMDs) within the TH transporters was achieved using the Simple Modular Architecture Research Tool (SMART) online software (Biobyte Solutions GmbH, Heidelberg, Germany), and the calculation of intra- and extracellular loops was performed manually. The prediction of PEST domains was performed using Mobyle@Pasteur version 1.0.4 online software (Pasteur Institute, Paris, France).

RESULTS

Isolation of the Full-length mct8 Transcript—We isolated a 1578-bp fragment of the *mct8* coding sequence, a 272-bp fragment of the 5′ UTR, and 557-bp 3′ UTR fragments (Fig. 1*A*). BLAT analysis (UCSC genome browser) revealed that the complete *mct8* mRNA (accession number JQ966311) consists of seven exons located on chromosome 14 in a region that was not fully sequenced in the latest version of the zebrafish genome (Sanger Institute, Zv9).

TH Transporter Proteins Are Well Conserved in Zebrafish and Mammals—Protein motif comparison of MCT8, MCT10, and OATP1C1 showed that the fish TH transporters share 12 similar TMDs, as well as similar intra- and extracellular loop spans, with their human orthologs (Fig. 1*B*). Confirming previous observations (22), the zebrafish protein sequence of MCT8 shares ∼60% identity with its human homolog, including a PEST domain at the N-terminal end. In addition, an arginine residue within TMD8 and an aspartate residue within TMD10, which were previously identified as being involved in substrate interaction in mammalian MCT8 (31, 32), are present in the
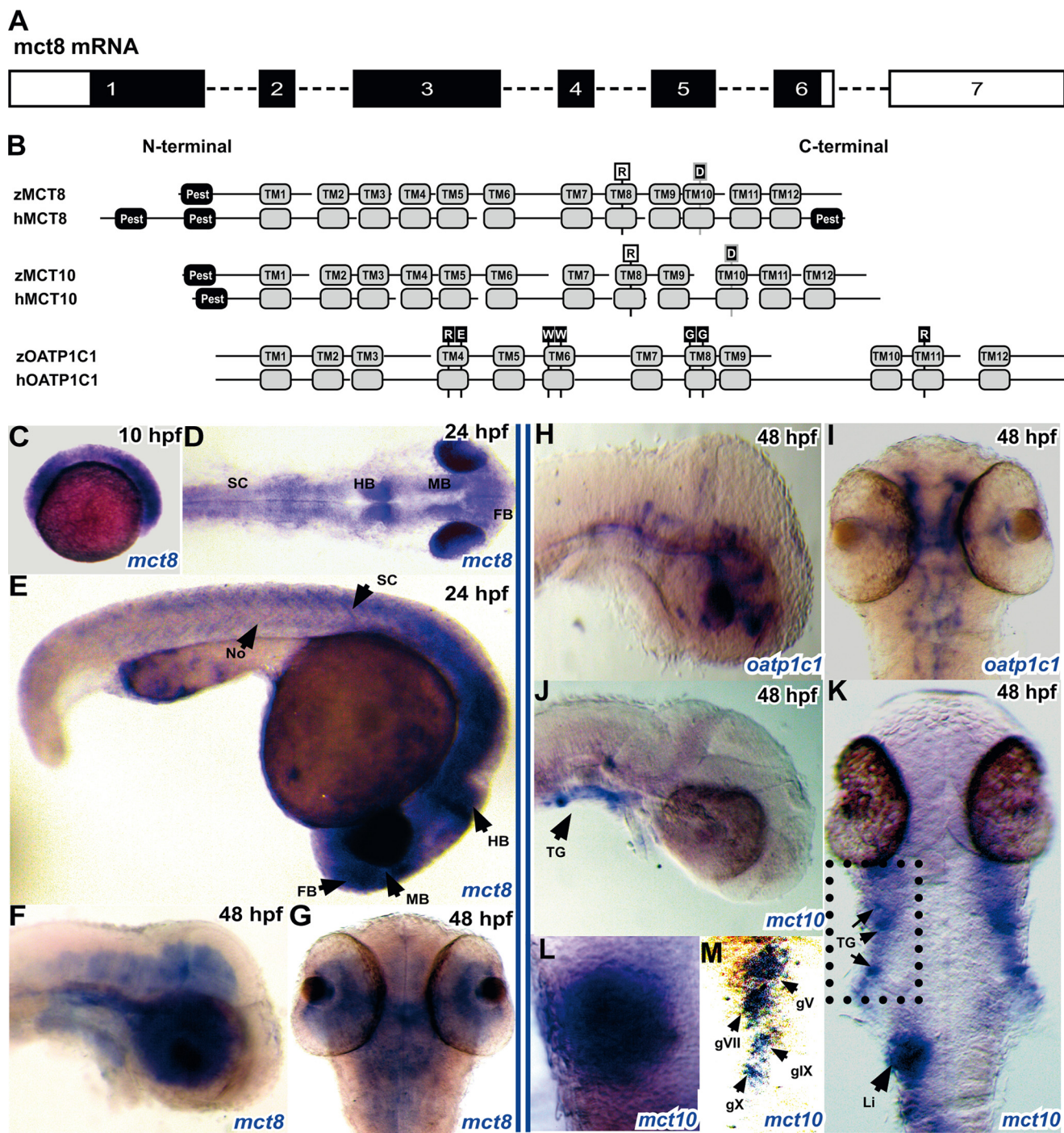
FIGURE 1. **The structure of *mct8* and expression pattern of TH transporters during development.** *A*, schematic illustration of the zebrafish *mct8* transcript. The zebrafish *mct8* mRNA consists of seven exons proportionally represented in the scheme. The *white box* in exon 1 represents the 5′ UTR, and the *white boxes* in exon 6 and exon 7 represent the 3′ UTR. *Black boxes* represent the coding sequence. *B,* sequence alignment of zebrafish and human MCT8, MCT10, and OATP1C1 proteins. *Gray boxes* represent the TMD. *Black boxes* represent predicted PEST domains. Known sensitive positions of TH transport are highlighted: human MCT8 (hMCT8) R445A is marked by a *black R* in a *white box* and a *black vertical bar* at TMD8; hMCT8 D498A is marked by a *white D in a black box* and a *gray vertical bar* at TMH10; the sensitive arginine and aspartate are conserved in the MCT8 and MCT10 groups. hOATP1C1-sensitive residues are marked by *white letters in black boxes* and *black bars*. *C,* lateral view of a 10-hpf embryo during bud stage shows ubiquitous expression of *mct8*. *D* and *E,* dorsal and lateral views of a 24-hpf embryo expressing *mct8* in the eyes and CNS, including the forebrain (*FB*), midbrain (*MB*), hindbrain (*HB*), and along the notochord (*No*) and spinal cord (*SC*). *F* and *G,* lateral and dorsal views of a 48-hpf embryo expressing *mct8* mainly in the CNS. *H* and *I,* lateral and dorsal views of 48-hpf embryos expressing *oatp1c1* in vasculature structures across the CNS. *J-M,* the expression pattern of *mct10* mRNA in a 48-hpf embryo. *J* and *K,* lateral and dorsal views of 48-hpf embryos expressing *mct10* in the liver (*Li*) and trigeminal ganglia (*TG*). *L,* close-up of the *black frame in K* showing *mct10* expression in the liver. *M,* close-up of the trigeminal ganglia shows *mct10* expression in the gV, gVII, gIX, and gX nuclei.

zebrafish MCT8. Similarly, zebrafish MCT10 holds both the conserved arginine and aspartate residues as well as a PEST domain at the N-terminal end, and shares 71% identity with its human ortholog. Furthermore, OATP1C1 of zebrafish (19) and humans share 58% identity, and sensitive residues, such as two tryptophan amino acids in TMD6, a couple of glycine residues

in TMD8, and an arginine within TMD11, are well conserved from fish to human (Fig. 1*B*). The conserved sequences and motifs of zebrafish and human MCT8, MCT10, and OATP1C1, suggest that the transport mechanism of TH is well conserved from fish to humans.

Expression Patterns of TH Transporters, mct8 Is Widely Expressed in the Nervous System—To characterize the spatial and temporal expression patterns of *mct8*, whole mount ISH was performed at several developmental stages. Ubiquitous *mct8* expression was observed during the bud stage in 10-hpf embryos (Fig. 1*C*). Later, at 24 hpf, the expression pattern of *mct8* was most abundant in the forebrain, midbrain, hindbrain, spinal cord, notochord, and eyes (Fig. 1, *D* and *E*). At 48 hpf, *mct8* expression was mainly observed in the brain and along the spinal cord (Fig. 1, *F* and *G*). Unlike the broad expression of *mct8* in the CNS, *oatp1c1* expression was restricted to vascular structures within the brain (Fig. 1, *H* and *I*), and expression of *mct10* was restricted to the liver and trigeminal ganglia (Fig. 1, *J–M*). These results suggest that MCT8 plays a general role during the development of the nervous system, and that other TH transporters are not likely able to fully compensate for MCT8 deficiency in zebrafish.

Isolation of a Functional mct8 Promoter and the Establishment of a Tg(mct8:EGFP) Transgenic Line—To visualize MCT8-positve cells in a live, developing animal, we sought to identify the zebrafish *mct8* promoter. An *in silico* approach was applied to identify conserved DNA regulatory sequences within putative *mct8* promoters. Comparison of our 5′ RACE analysis with available genomic data revealed that the start codon is located within the first exon in zebrafish and mammals (Fig. 1*A*). Therefore, fragments of 2000 bp upstream to the ATG of zebrafish, mouse, rat, and human, were analyzed. Conserved transcription factor binding sites for the purine-rich single-stranded DNA-binding protein α (PURA, $p < 1.4E-04$), the Huntington disease gene-regulatory region binding proteins (HDBP, $p < 5.77E-04$), and GATA ($p < 0.05$) were found in all four putative promoters (Fig. 2*A*). To functionally test the zebrafish *mct8* promoter *in vivo*, a 2000-bp genomic fragment (Fig. 2*B*, accession number JQ966310), located upstream of the start codon, was cloned upstream of an EGFP. The *pT2-mct8:EGFP* construct was microinjected into one-cell stage embryos. At 24 hpf, ubiquitous mosaic EGFP expression was observed, suggesting that the 2000-bp promoter can drive gene expression *in vivo*. To test whether this promoter can drive specific expression in all *mct8*-positive cells, a stable *Tg(mct8:EGFP)* transgenic line was established (Fig. 2, *C–I*). At 24 hpf, this *Tg(mct8:EGFP)* fish expressed EGFP mainly in the forebrain, midbrain, hindbrain, along the spinal cord and notochord, and in the eyes (Fig. 2, *C–E*). Expression in the notochord gradually disappeared during development. High resolution imaging revealed expression in various tissues, including cells along the spinal cord and notochord (Fig. 2*F*), epithelial cells above the otic vesicle (Fig. 2*G*), the choroid plexus (Fig. 2*H*), and olfactory bulbs (Fig. 2*I*). This expression pattern was consistent at least until 11 days post-fertilization (dpf).

mct8 Is Expressed in the Vascular System—As *mct8* is a hormone transporter, we monitored its expression in the vascular system. At 3 dpf, EGFP expression was observed in vessel-like
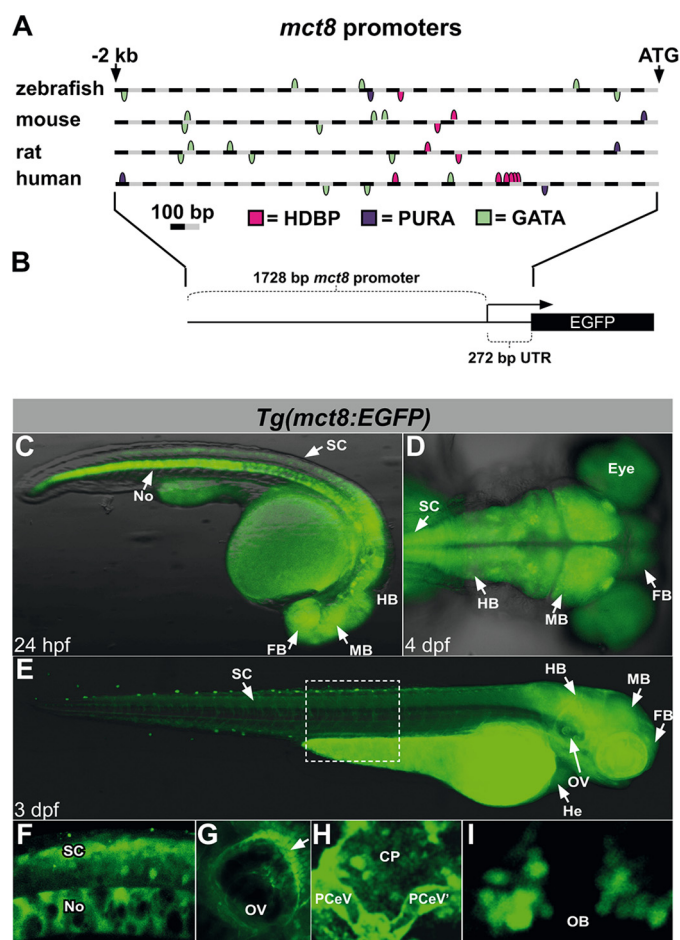

FIGURE 2. **Isolation of a functional *mct8* promoter and generation of a *Tg(mct8:EGFP)* stable transgenic fish.** *A,* bioinformatic analysis of putative 2000-bp orthologous *mct8* promoters from zebrafish, mouse, rat, and human. *Oval color*-coded marks drawn *above* or *below the black and gray bars* indicate the sense or antisense direction of the transcription-factor binding sites, respectively. *Purple* represents binding sites for the purine-rich single-stranded DNA-binding protein α (*PURA*). *Pink* represents binding sites for Huntington disease gene regulatory region binding proteins (HDBP). *Green* represents putative binding sites for GATA. *B,* schematic illustration of the pT2-*mct8*:EGFP DNA construct that was used to generate the *Tg(mct8:EGFP)* transgenic line. *C-I, Tg(mct8:EGFP)* transgenic larvae. *C,* lateral view of a 24-hpf embryo. EGFP expression driven by the *mct8* promoter is observed in the CNS, including the forebrain (*FB*), midbrain (*MB*), hindbrain (*HB*), and along the spinal cord (*SC*). EGFP is also expressed in the eyes and in the notochord (*No*). *D,* dorsal view of the head of a 4-dpf larva. *E,* lateral view of a 3-dpf larva. EGFP is expressed in the CNS, eyes, otic vesicle (*OV*), and heart (*He*). *F,* lateral view of the spinal cord (*SC*) and the notochord (*No*) of a 48-hpf embryo. *G,* lateral view of the otic vesicle of a 4-dpf larva. *White arrows* point to epithelial cells located above the otic vesicle. *H,* dorsal view of a 4-dpf larva. EGFP expression is observed in the posterior cerebral veins (*PCeV*) and in cells within the choroid plexus (*CP*). *I,* dorsal view of the olfactory bulbs (*OB*) of a 4-dpf larva.

structures in *Tg(mct8:EGFP)* larvae (Fig. 2*E*, *white dashed box*). To examine this expression pattern, *Tg(mct8:EGFP)* and *Tg(fli:DsRED)* fish were crossed, and their progeny were imaged by confocal microscopy. In the *Tg(fli:DsRED)* line, blood and lymphatic vessels were marked with red fluorescent protein (30). In the *Tg(mct8:EGFP/fli:DsRED)* double transgenic larvae, EGFP and DsRED colocalized in trunk vessels, specifically, in the dorsal aorta, the posterior cardinal vein, and the intersegmental vessels (Fig. 3, *A–C*). In addition, colocalization was observed in the thoracic duct of the lymphatic system. To check whether *mct8* is expressed in blood vessels in the brain, imaging was
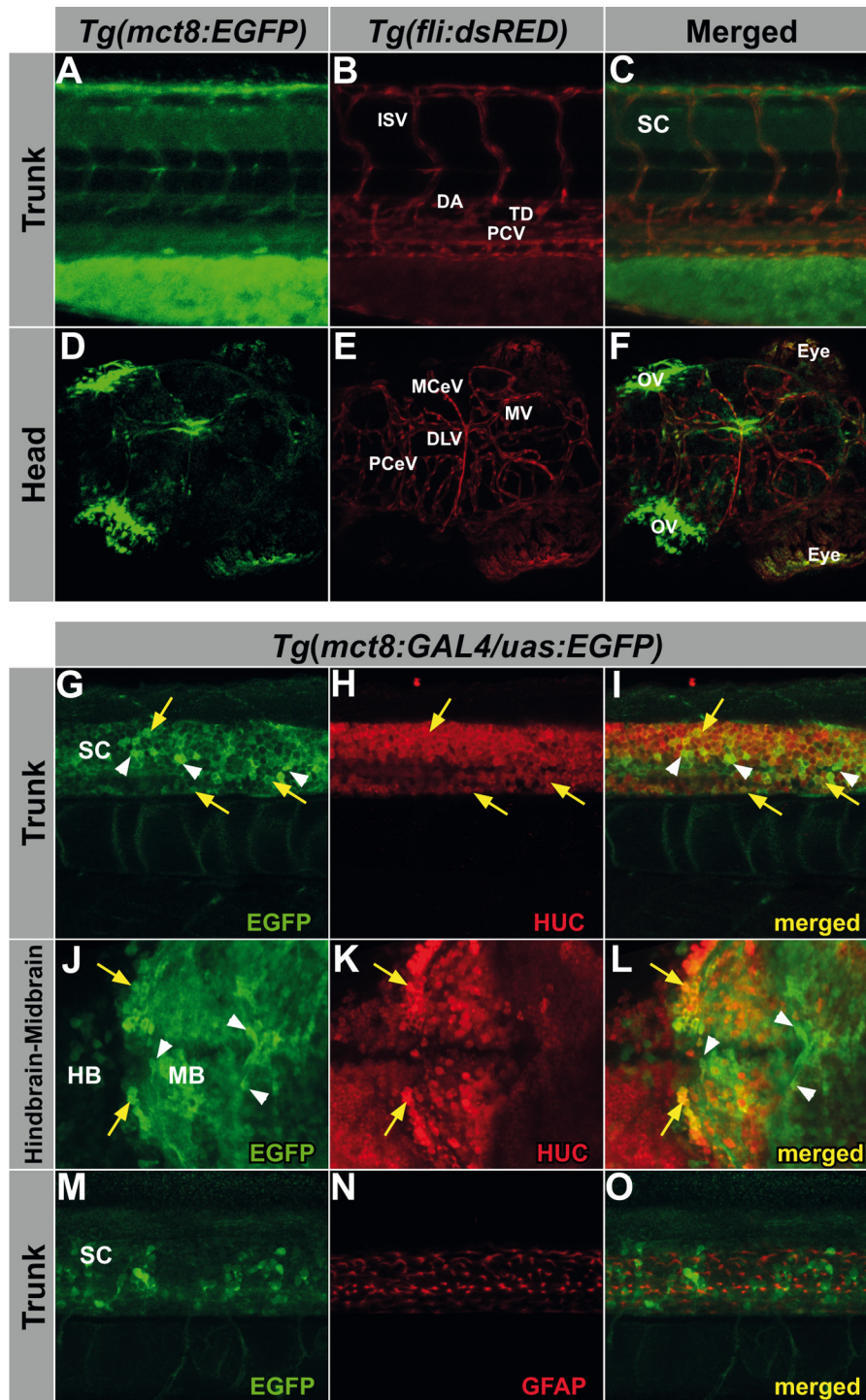
FIGURE 3. **mct8 is expressed in the vascular system and in neurons.** Colocalization experiments on larvae (pointing to the right). *A-F*, confocal imaging of a 5-dpf live *Tg*(*mct8:EGFP*)/*Tg*(*fli:dsRED*) double-transgenic larvae showing colocalization of *mct8* (*green*) and the vasculature specific *fli* marker (*red*). *A-C*, magnification of the region marked in a *white dashed frame* in Fig. 2*E*. Lateral view of the trunk. Colocalization is observed in the intersegmental vessels (*ISV*), dorsal aorta (*DA*), the posterior cardinal vein (*PCV*), and the thoracic duct (*TD*), but not in the spinal cord (*SC*). *D-F*, dorsal view of the head. Colocalization is observed in the midbrain veins (*MV*), middle cerebral veins (*MCeV*), dorsal longitudinal veins (*DLV*), and the posterior cerebral veins (*PCeV*), but not in the otic vesicle (*OV*) and choroid plexus (*CP*). The *yellow* signal observed in the eyes is due to autofluorescence of the eye pigments. *G-O*, confocal imaging of double-staining immunohistochemistry in *Tg*(*mct8:GAL4/uas:EGFP*) 3-dpf larvae. *G-L*, immunoreactive stained cells in larvae showing colocalization of *mct8* promoter-driven EGFP (*green*) and the neuron-specific HUC marker (*red*) in the trunk (lateral view, *G-I*) and in the brain (dorsal view of the midbrain (*MB*), hindbrain (*HB*), and the midbrain-hindbrain boundary, *J-L*). *Yellow arrows* point to EGFP and HUC colocalized neurons, and *white arrowheads* point to non-colocalized EGFP cells, which are characterized by *oval shapes* and short projections, and are similar to oligodendrocytes. *M-O*, immunoreactive EGFP (*green*) and GFAP (*red*) stained cells do not colocalize in the trunk (lateral view), indicating that *mct8* is not expressed in astrocytes within the trunk.

performed in the head of *Tg(mct8:EGFP/fli:DsRED)* larvae (Fig. 3, *D–F*). Notably, colocalized expression was detected in the midbrain veins, the middle cerebral veins, the dorsal longitudinal vein, and the posterior cerebral veins (33). These results indicate that MCT8 is expressed in both blood and lymphatic vascular systems and is likely involved in TH transport into the CNS.

mct8 Is Expressed in Neurons and Neuron-supporting Cells—To specifically identify the cells that express *mct8* in the CNS, immunofluorescence double labeling assays were conducted in *Tg(mct8:GAL4/uas:EGFP)* fish, which demonstrated more robust EGFP expression levels than the *Tg(mct8:EGFP)* line. Antibodies against EGFP and the HUC protein, a marker of developing neurons (34), or the glial fibrillary acidic protein (GFAP), a marker of astrocytes (35), were used. At 3 dpf, EGFP immunoreactive cell bodies were detected in the brain and along the spinal cord, where they colocalized with HUC-positive neurons (Fig. 3, *G–L*). In contrast, EGFP immunoreactive cell bodies were not colocalized with GFAP-positive astrocytes in the spinal cord (Fig. 3, *M–O*). These results indicate that *mct8* is expressed in neurons but not in astrocytes. Furthermore, EGFP immunoreactive cells were observed in cells that were not stained by either HUC or GFAP antibodies (Fig. 3m *G, I, J, L, M*, an *O*). The location and shape of these cells was similar to SOX10-positive oligodendrocyte; the myelin-forming cells (36, 37). These results suggest that MCT8 transports THs from the blood vessels into oligodendrocytes and neurons, and regulates myelination and neuron development.

Establishment of MCT8-deficient fish, the Expression of TH-related Genes Is Not Altered—To establish an MCT8-deficient model in zebrafish, MCT8 was knocked down (KD) by injecting two different MOs into one-cell stage embryos. The *mct8*(UTR)MO was designed to block translation and the *mct8*(E2I2)MO was designed to interfere with the splicing of the second exon/intron. *In vivo* and *in vitro* experiments confirmed that both MOs are able to efficiently and specifically knockdown MCT8 (Figs. 4*A* and 5, respectively). To examine the effect of MCT8 knockdown on the TH endocrinological system, spatial and quantitative expression assays were performed on the three deiodinases (*dio1, -2*, and *-3*) (18, 20) and the *thyroid stimulating hormone β* (*tshβ*) (38). The deiodinases selectively remove iodide from thyroxine and its derivatives, thus activating or inactivating THs. TSH is secreted by the pituitary and regulates the function of the thyroid gland. TSH consists of α- and β-subunits (39, 40). As the localization of the deiodinase genes had not been previously described in zebrafish, the spatial expression of the three deiodinases was monitored using whole mount ISH (Fig. 4, *B–D*). At 48 hpf, *dio1* was strongly expressed in the liver and weakly expressed in the head. *dio2* was specifically expressed in the thyroid gland, and *dio3* was expressed primarily in the pronephros. Next, at 48 hpf, total mRNA was extracted from *mct8*(E2I2)MO-, *mct8*(UTR)MO-, or control MO-injected embryos, and the expression levels of *dio1, dio2, dio3*, and *tshβ* were quantified using quantitative RT-PCR. KD of MCT8 did not affect the expression levels of the deiodinases and *tshβ* (Fig. 4*E*). These results show that zebrafish MCT8 does not regulate deiodinase and *tshβ* gene expression in the whole larvae at early develop-
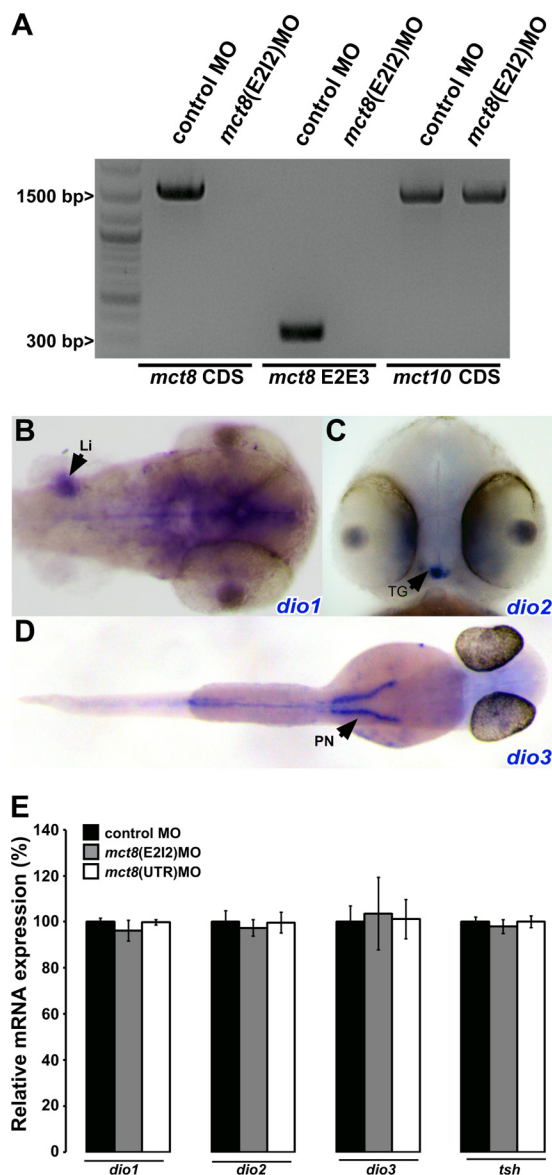

FIGURE 4. **The mRNA expression levels of thyroid-related genes were not affected by the knockdown of MCT8.** *A,* gel analysis of *mct8* cDNA shows that the injection of *mct8*(E2I2)MO, designed to target the Exon 2-Intron 2 boundary, effectively and specifically knocks down *mct8* mRNA expression in 48-hpf larvae. cDNA was prepared from total mRNA of control MO- or *mct8*(E2I2)MO-injected embryos. A fragment of 1578 bp of the *mct8* coding sequence (*mct8* CDS) and a fragment of ~400 bp containing a fragment of exon 2 and exon 3 (*mct8* E2E3), were PCR amplified in control MO-injected embryos but not in *mct8*(E2I2)MO-injected embryos. The specific knockdown of *mct8* did not affect the expression of *mct10* CDS, which was present in both control MO- and *mct8*(E2I2)MO-injected embryos. *B-D*, whole mount ISH experiments show the spatial mRNA expression of *deiodinase1* (*dio1*), *deiodinase2* (*dio2*), and *deiodinase3* (*dio1*) in 48-hpf embryos. *B,* dorsal view. *dio1* is expressed in the liver (*Li*) and brain. *C,* ventral view. *dio2* is specifically expressed in the thyroid gland (*TG*). *D,* dorsal view. *dio3* is expressed in the pronephros (*PN*). *E,* quantification by quantitative RT-PCR of relative mRNA expression levels of *dio1, dio2, dio3*, and *tsh*. cDNA was produced from whole 48-hpf embryos injected with control MO (*black bars*), *mct8*(E2I2)MO (*gray bars*), or *mct8*(UTR)MO (*white bars*). Values are represented as mean ± S.E.

mental stages. Nevertheless, MCT8 may affect these enzymes in specific tissues or at the protein and protein-activity levels.

Knockdown of mct8 Alters the Development of Zebrafish Embryos—To study the effect of MCT8 knockdown on the morphology and development of zebrafish embryos,
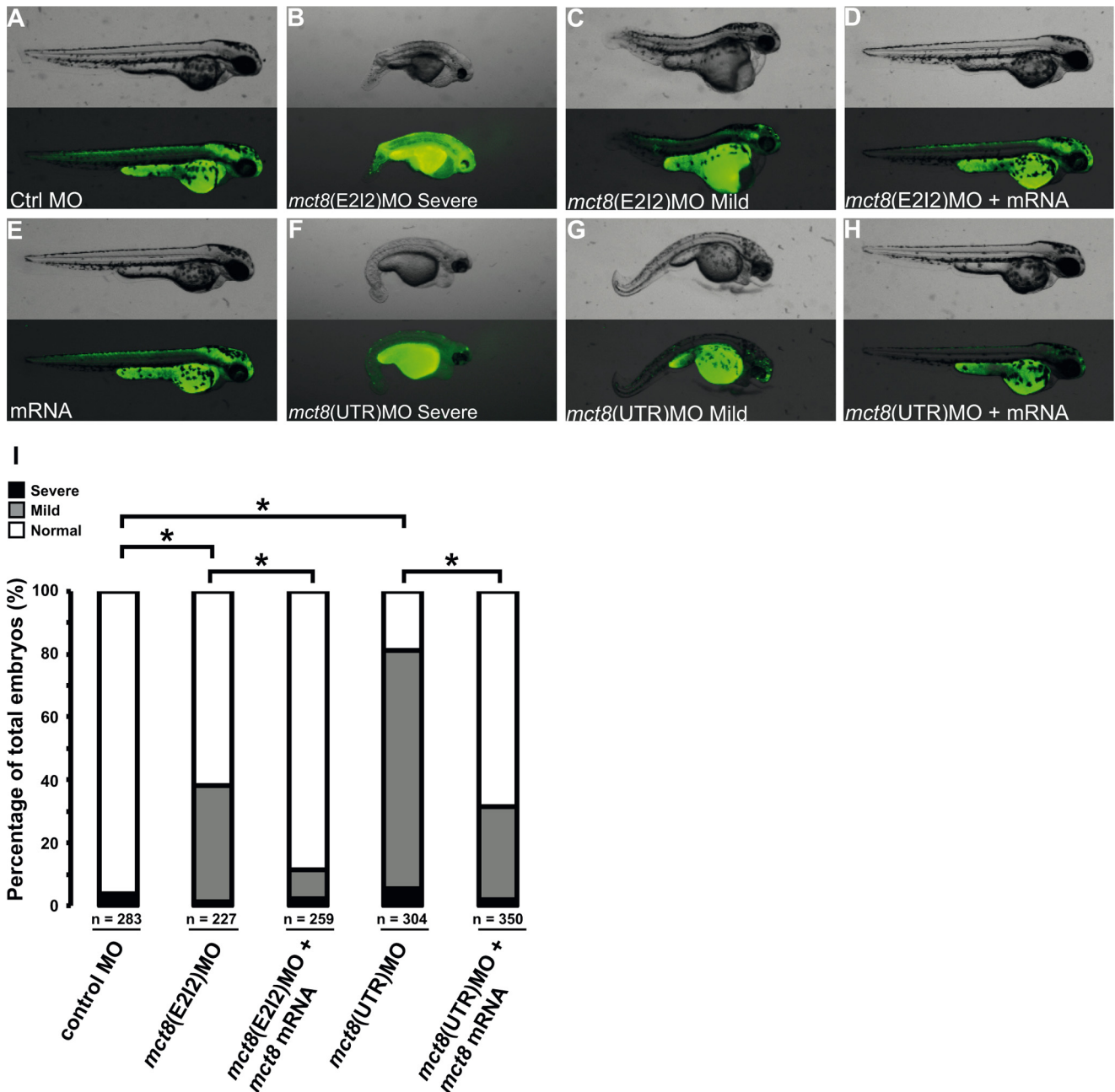
FIGURE 5. **Knockdown of MCT8 alters the development of the zebrafish embryo.** *A-H,* lateral views (anterior to the *right* and dorsal at the *top*) of 72-hpf *Tg*(*mct8:EGFP*) embryos injected with control MO, *mct8*(E2I2)MO, *mct8*(E2I2)MO+*mct8* mRNA, *mct8*(UTR)MO, *mct8*(E2I2)MO+*mct8* mRNA, and *mct8* mRNA. Representative embryos with normal (*A*, *D*, *E*, and *H*), severe (*B* and *F*), and mild (*C* and *G*) phenotypes are shown. Injection of *mct8* mRNA alone did not cause abnormal development and rescued the altered development phenotype observed in MO-injected embryos. *I,* embryos injected with MOs or MOs+*mct8* mRNA were sorted according to the morphological criteria shown in *A-H*. The percentage of embryos from each phenotype is presented. The numbers of *mct8*(E2I2)MO- and *mct8*(UTR)MO-injected embryos demonstrating altered development were significantly ($p < 1 \times e^{-20}$) higher than the number of altered control MO-injected embryos. In rescue experiments, the injection of *mct8* mRNA into MOs-injected embryos significantly ($p < 1 \times e^{-20}$) reduced the number of embryos demonstrating altered morphology. Statistical significance was determined by χ square tests and by comparing the distribution of normal, mild, and severely altered development phenotypes.

mct8(E2I2)MO, *mct8*(UTR)MO, or control MO were independently injected into one-cell stage *Tg*(*mct8:EGFP*) embryos. MO-injected embryos exhibited a normal survival rate (above 95% at 24 hpf). Notably, at 48 hpf, the injection of both *mct8*(E2I2)MO and *mct8*(UTR)MO caused an altered developmental phenotype, characterized by small eyes, decreased pigmentation, pericardial edema, and perturbed trunk and tail development (Fig. 5). A large portion of the MO-injected embryos exhibited a mild phenotype and their morphology was only slightly altered. The number of embryos displaying mild to severe altered development was significantly higher compared with the control MO ($p < 1Xe^{-20}$, $\chi^2 = 10857.492$, df = 2 and $p < 1Xe^{-20}$, $\chi^2 = 36118.169$, df = 2, respectively). Moreover, because MCT8-expressing cells were fluorescently labeled, we noticed that the brain, spinal cord, and notochord were severely deformed (Fig. 5, *B*, C, *F*, and *G*). These results suggest that MCT8 is necessary for normal embryonic development.

To confirm that this altered development of the nervous system is specific to MCT8 deficiency, we performed rescue experiments. We initially injected *mct8* mRNA into *Tg(mct8:EGFP)* one-cell stage embryos, and no apparent morphological changes were observed (Fig. 5*E*). Co-injection of *mct8* mRNA with *mct8*(E2I2)MO or *mct8*(UTR)MO rescued the altered developmental phenotype (Fig. 5, *D* and *H*). Following co-injections of each MO with *mct8* mRNA, a significantly lower percentage of embryos displayed an altered developmental phenotype (Fig. 5, *I*, $p < 1Xe^{-20}$, $\chi^2 = 5392.65$, df = 2 for the *mct8*(E2I2)MO *versus* *mct8*(E2I2)MO+*mct8* mRNA; $p < 1Xe^{-20}$, $\chi^2 = 16290.365$, df = 2 for the *mct8*(UTR)MO *versus* *mct8*(UTR)MO+*mct8* mRNA). These results indicate that *mct8* mRNA can rescue the developmental defects caused by MCT8-KD, and that the MO-mediated phenotype is a specific result of MCT8 deficiency.

Knockdown of mct8 Specifically Alters Neural Development in Zebrafish Embryos—To investigate the function of MCT8 in specific tissues, whole mount ISH and immunohistochemistry experiments were performed in MO-injected embryos that demonstrated mild morphological phenotype. Because MCT8 deficiency in human patients affects muscle tone, the morphology and development of the muscles were studied. At 24 hpf, the expression pattern of *myod* mRNA, a marker for muscle development (24), was monitored in control MO- and *mct8*(E2I2)MO-injected embryos. Although the trunk was mildly deformed (as described above, Fig. 5), *myod* expression levels and muscle morphology were mostly similar in *mct8*(E2I2)MO-injected and wild-type embryos (Fig. 6, *A* and *B*). Similarly, at 5 dpf, the morphology of the vascular system in *mct8*(E2I2)MO-injected *Tg(fli:DSRED)* larvae was mostly intact (Fig. 6, *C* and *D*). In contrast, in the CNS, the number of MCT8-positive cells was reduced and the cell organization was altered in the hindbrain, midbrain-hindbrain boundary, midbrain (Fig. 6, *G* and *H*), and spinal cord (Fig. 6, *E* and *F*) of *mct8*(E2I2)MO-injected 2 dpf larvae. These results strongly suggest that loss of MCT8 does not affect the development of muscles and vessel; however, it plays an essential role in the development of the CNS. Altogether, these experiments establish the zebrafish as a model for studying the role of MCT8 and the mechanisms underlying AHDS.

DISCUSSION

The effect of MCT8 on neural development and its role in the psychomotor retardation AHDS is not clear. To study the function of MCT8, we developed an MCT8-deficent zebrafish. This simple model provides genetic and imaging tools that are unique among all vertebrate models. To characterize the spatial and temporal expression of *mct8*, we cloned the complete *mct8* mRNA and performed whole mount ISH on developing embryos. We found that *mct8* was ubiquitously expressed at 10 hpf. As MCT8 transports THs, and maternal THs are important for early brain development (41, 42), the observed *mct8* expression implies that MCT8 may allow the accumulation of active THs, even at early developmental stages. At 1–2 dpf, *mct8* was mainly expressed in the CNS, specifically in the forebrain, midbrain, hindbrain, and along the spinal cord and notochord. This expression pattern partially recapitulates the
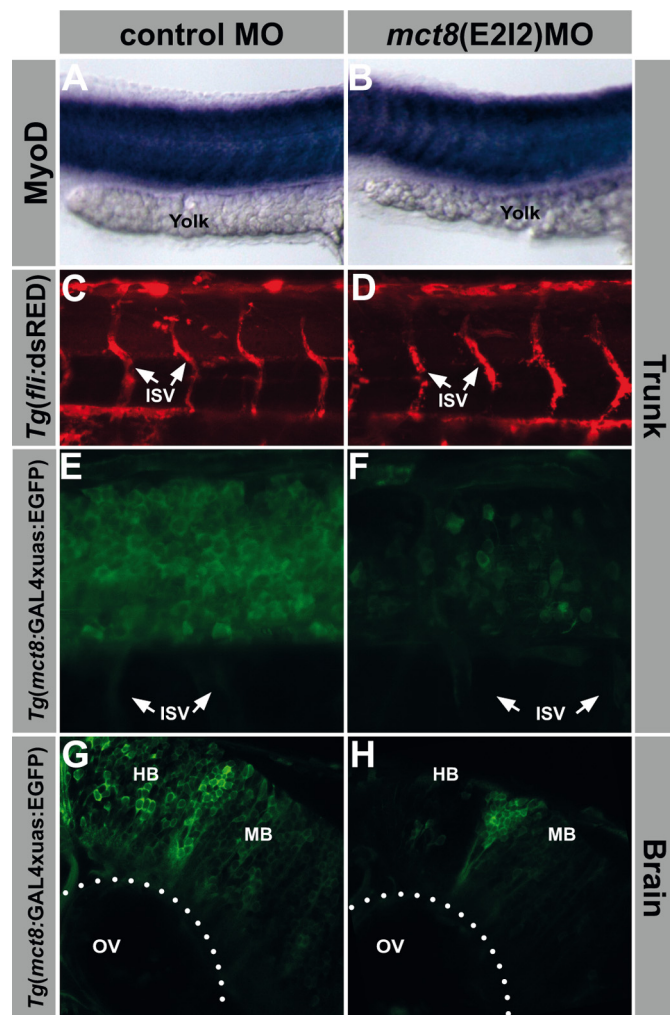

FIGURE 6. **Knockdown of MCT8 specifically alters the development of the nervous system.** Lateral view (head pointing to the right) of 24 hpf (*A* and *B*), 5 dpf (*C* and *D*), and 2 dpf (*E-H*) control (*A*, *C*, *E*, and *G*) and *mct8*(E2I2)MO-injected (*B*, *D*, *F*, and *H*) embryos and larvae. *A* and *B*, whole mount ISH assays using mRNA probe against the muscle-specific marker *myod* in 24 hpf larvae. *C* and *D*, the trunk of 5 dpf *Tg(fliLDsRED)* transgenic larvae. *White arrows* denote intersegmental vessels (*ISV*). *E-H*, immunohistochemistry assays using antibody against *mct8* promoter-driven EGFP in the trunk (*E* and *F*) and brain (*G* and *H*) of 2 dpf *Tg(mct8:GAL4/uas:EGFP)* transgenic larvae. The location of the otic vesicle (*OV*) is marked with a *white dotted line*. *MB*, midbrain; *HB*, hindbrain.

expression profile of *mct8* in the mammalian nervous system (43, 44). These results suggest that MCT8 plays a general role in early developmental stages and is possibly a key regulator during the development of the nervous system.

To understand a broader view of zebrafish TH transport, we also performed whole mount ISH using probes of other TH transporters. Although *mct8* was widely expressed in the CNS, *oatp1c1* expression was restricted to vasculature structures within the brain. Similarly, in rodents, *oatp1c1* shows a strong expression in brain endothelial cells and in choroid plexus structures (6, 12, 45). MCT10, which is thought to act in the liver, intestine, kidneys, and growth plate chondrocytes in mammals (6, 46, 47), was observed in the liver and the trigeminal ganglia in zebrafish. Recently, OATP1C1 was implicated as compensating for the lack of MCT8 in MCT8-knock-out mice (12, 48). The distinct expression patterns of *oatp1c1* and *mct10*

suggest that, in contrast to the mouse model and as is the case in humans, they are not likely able to fully compensate for MCT8 deficiency in zebrafish.

To further study the expression pattern of MCT8 in live developing animals, a *Tg*(*mct8:EGFP*) stable transgenic line was generated. The EGFP pattern was similar to endogenous *mct8* expression, thus, this line provides a platform for the imaging of MCT8-positive cells in live animals. High magnification imaging revealed EGFP expression in various cell types, including epithelial cells above the otic vesicle, in the olfactory bulb, and in the choroid plexus. This expression pattern is consistent with previous reports on chicken embryos (42, 49) and mammals (43). The expression pattern in the choroid plexus suggests that MCT8 may play a role in the transport of THs into the cerebrospinal fluid. Furthermore, double immunofluorescence assays revealed that *mct8* colocalized with HUC in neurons of the brain and spinal cord but not with GFAP in astrocytes, consistent with the *mct8* expression pattern in mice (6, 43, 50). In addition, *mct8* expression was observed in oval cell bodies with short projections that did not express both HUC and GFAP markers. Because the structure and the location of these cells are similar to *sox10* expressing cells (36, 37), they are likely to be oligodendrocytes. Similarly, in mammals, *mct8* mRNA and protein were present in oligodendroglial cells derived from mice (50). These results suggest a role for MCT8 in the uptake of THs in neurons and oligodendrocytes. Thus, MCT8 regulates the maintenance and development of neurons. Because a key role of oligodendrocytes is to produce a myelin sheath, MCT8 may also be involved in the myelination of neurons. This hypothesis is consistent with recent reports of delayed myelination in AHDS patients (51). Future studies on live developing zebrafish are required to understand the role of MCT8 in neuron maintenance and myelination.

In live *Tg*(*mct8*:*EGFP*/*fli*:*DsRED*) double transgenic larvae, co-expression of EGFP and DsRED was observed in both the blood and lymphatic vascular systems. Thus, MCT8 is likely to play a key role in the transport of THs across the vessel membrane and into the nervous system. Colocalization of EGFP and DsRed was also observed in vessels surrounding the brain; however, not in the region where zebrafish blood-brain barrier was identified (52). This finding is consistent with previous reports on chickens (42). In contrast, in rodents, MCT8 mRNA and protein were observed in the blood-brain barrier (53), suggesting that MCT8 is not directly involved in TH transport across the blood-brain barrier in non-mammalian vertebrates. Our expression studies suggest that, as is the case in mammals (6, 12, 48), OATP1C1 can function in zebrafish blood-brain barrier, and MCT8 can regulate the transport of THs from the blood to the nervous system in distinct regions.

EGFP expression in the *Tg*(*mct8:EGFP*) closely mimics the pattern of expression of the endogenous *mct8* mRNA, indicating that the *mct8* promoter is functional in live animals. The effect of MCT8 on gene transcriptional regulation was previously investigated in fibroblasts derived from AHDS patients (54); however, very little is known about the transcriptional regulation of the *mct8* gene. An *in vitro* study performed on mouse cells revealed the presence of a putative *mct8* core promoter containing an SP1 binding site that might be important for *mct8* transcriptional regulation (55). Here, we isolated, for the first time, a *mct8* promoter that contains distinct regulatory regions and that is functional *in vivo*. Interestingly, we found that binding sites for the PURA, HDBP, and GATA transcription factors are conserved from fish to humans. Both the PURA and HDBP transcription factors have previously been associated with the development of the nervous system (56, 57), and GATA is commonly present in regulatory elements of blood-related genes (58). The presence of these putative binding sites is consistent with the expression observed in the nervous and vascular systems, respectively. Promoter-bashing experiments will clarify the specific role of these putative elements in *mct8* transcriptional regulation in animal models and humans. The zebrafish promoter and the transgenic lines will serve as powerful tools for functional promoter analysis in the future, thereby providing a platform for the identification of novel transcriptional mechanisms that regulate *mct8* expression. Importantly, the promoter isolation in zebrafish could likely aid in the identification of a functional *mct8* promoter in humans. This benefit will be a critical step toward applying tissue-specific gene therapy in AHDS patients.

Knockdown of MCT8 did not affect the expression levels of key TH genes: the deiodinases and *tshβ*. These results suggest that although the zebrafish MCT8 is able to uptake TH in cell lines (22), it does not regulate deiodinase and *tshβ* gene expression at early developmental stages. In contrast, in MCT8-knock-out mice, the mRNA levels of *dio1* in the liver and *dio2* in the cerebrum significantly increased (9). This discrepancy between zebrafish and mice could be explained by the relatively early developmental stage at which larvae were sampled. The establishment of a MCT8-mutant zebrafish will enable sampling of mRNA from specific tissues in adults rather than from whole larvae. Alternatively, it is possible that protein activity, rather than transcription, was affected by the KD of zebrafish MCT8. Nevertheless, because MCT8-KD had a major effect on embryonic development, it cannot be excluded that MCT8 play an elusive role that is independent of its function as a TH transporter.

The establishment of MCT8-deficient mouse models has significantly advanced our understanding of the endocrinological phenotype linked to AHDS, yet these murine models do not display obvious neurological and psychomotor deficiencies (9). Additional non-mammalian models, such as chicken and frog, were used to study the role of MCT8 in TH transport (2, 42). However, although the role of MCT8 in regulating the TH endocrinological system is well characterized, the cause for the AHDS neurological symptoms and the mechanisms underlying MCT8 deficiency remain poorly understood. Here, we showed that KD of MCT8 results in a mild to severe altered developmental phenotype. The injection of both MCT8-MOs into embryos resulted in similar phenotypes. Moreover, the use of the *Tg*(*mct8:EGPF*) transgenic line revealed that the development of *mct8*-expressing cells was altered and caused deformed brain, spinal cord, and notochord. High magnification confocal imaging revealed that KD of MCT8 reduced the number and altered the organization of neural cells in the brain and spinal cord. This robust phenotype may result from insufficient levels of THs in the cerebrospinal fluid, neurons, and glial cells. On

the other hand, the development of muscles and vessels was mostly intact and only a weak malformation was observed in these tissues. This neural-specific phenotype suggests that MCT8 plays a key role in the development of the nervous system. In turn, the altered nervous system may cause severe physiological and behavioral abnormalities.

The role of MCT8 was further studied using the overexpression of mRNA. The injection of *mct8* mRNA alone, which results in homogenous and ubiquitous expression in the whole embryo, did not seem to cause any abnormal developmental defects. However, it was able to efficiently rescue the phenotype of MCT8-MO-injected embryos. These results strongly suggest that the described phenotype is specific to MCT8 deficiency and indicate that MCT8 does not have a toxic effect on non-MCT8 expressing cells, thus addressing important questions for gene therapy.

This study establishes the zebrafish as a promising model to study the role of MCT8 and the mechanisms underlying AHDS. Future studies using live time lapse imaging (13) in MCT8-mutant embryos will enable testing fine changes in neuronal structures and circuit connectivity throughout the developmental stages. Furthermore, as the zebrafish has been increasingly used as a high-throughput genetic model organism for pharmacological screens (59, 60), this study may be used as a platform for future screens of therapeutic reagents that may compensate for MCT8 deficiency and aid in the treatment of AHDS patients.

REFERENCES

1. Yen, P. M. (2001) Physiological and molecular basis of thyroid hormone action. *Physiol. Rev.* **81,** 1097–1142
2. Friesema, E. C., Ganguly, S., Abdalla, A., Manning Fox, J. E., Halestrap, A. P., and Visser, T. J. (2003) Identification of monocarboxylate transporter 8 as a specific thyroid hormone transporter. *J. Biol. Chem.* **278,** 40128–40135
3. Friesema, E. C., Jansen, J., Jachtenberg, J. W., Visser, W. E., Kester, M. H., and Visser, T. J. (2008) Effective cellular uptake and efflux of thyroid hormone by human monocarboxylate transporter 10. *Mol. Endocrinol.* **22,** 1357–1369
4. Kim, D. K., Kanai, Y., Chairoungdua, A., Matsuo, H., Cha, S. H., and Endou, H. (2001) Expression cloning of a Na^+-independent aromatic amino acid transporter with structural similarity to H^+/monocarboxylate transporters. *J. Biol. Chem.* **276,** 17221–17228
5. Tohyama, K., Kusuhara, H., and Sugiyama, Y. (2004) Involvement of multispecific organic anion transporter, Oatp14 (Slc21a14), in the transport of thyroxine across the blood-brain barrier. *Endocrinology* **145,** 4384–4391
6. Heuer, H., and Visser, T. J. (2009) Minireview. Pathophysiological importance of thyroid hormone transporters. *Endocrinology* **150,** 1078–1083
7. Brockmann, K., Dumitrescu, A. M., Best, T. T., Hanefeld, F., and Refetoff, S. (2005) X-linked paroxysmal dyskinesia and severe global retardation caused by defective *MCT8* gene. *J. Neurol.* **252,** 663–666
8. Friesema, E. C., Grueters, A., Biebermann, H., Krude, H., von Moers, A., Reeser, M., Barrett, T. G., Mancilla, E. E., Svensson, J., Kester, M. H.,

8. Kuiper, G. G., Balkassmi, S., Uitterlinden, A. G., Koehrle, J., Rodien, P., Halestrap, A. P., and Visser, T. J. (2004) Association between mutations in a thyroid hormone transporter and severe X-linked psychomotor retardation. *Lancet* **364,** 1435–1437
9. Dumitrescu, A. M., Liao, X. H., Weiss, R. E., Millen, K., and Refetoff, S. (2006) Tissue-specific thyroid hormone deprivation and excess in monocarboxylate transporter (mct) 8-deficient mice. *Endocrinology* **147,** 4036–4043
10. Trajkovic, M., Visser, T. J., Mittag, J., Horn, S., Lukas, J., Darras, V. M., Raivich, G., Bauer, K., and Heuer, H. (2007) Abnormal thyroid hormone metabolism in mice lacking the monocarboxylate transporter 8. *J. Clin. Invest.* **117,** 627–635
11. Heuer, H., and Visser, T. J. (2012) The pathophysiological consequences of thyroid hormone transporter deficiencies. Insights from mouse models. *Biochim. Biophys. Acta,* in press
12. Mayerl, S., Visser, T. J., Darras, V. M., Horn, S., and Heuer, H. (2012) Impact of Oatp1c1 deficiency on thyroid hormone metabolism and action in the mouse brain. *Endocrinology* **153,** 1528–1537
13. Appelbaum, L., Wang, G., Yokogawa, T., Skariah, G. M., Smith, S. J., Mourrain, P., and Mignot, E. (2010) Circadian and homeostatic regulation of structural synaptic plasticity in hypocretin neurons. *Neuron* **68,** 87–98
14. Stiebel-Kalish, H., Reich, E., Rainy, N., Vatine, G., Nisgav, Y., Tovar, A., Gothilf, Y., and Bach, M. (2012) Gucy2f zebrafish knockdown. A model for Gucy2d-related leber congenital amaurosis. *Eur. J. Hum. Genet.* **20,** 884–889
15. Vatine, G., Vallone, D., Appelbaum, L., Mracek, P., Ben-Moshe, Z., Lahiri, K., Gothilf, Y., and Foulkes, N. S. (2009) Light directs zebrafish period2 expression via conserved D and E boxes. *PLoS Biol* **7,** e1000223
16. Porazzi, P., Calebiro, D., Benato, F., Tiso, N., and Persani, L. (2009) Thyroid gland development and function in the zebrafish model. *Mol. Cell. Endocrinol.* **312,** 14–23
17. Yan, W., Zhou, Y., Yang, J., Li, S., Hu, D., Wang, J., Chen, J., and Li, G. (2012) Waterborne exposure to microcystin-LR alters thyroid hormone levels and gene transcription in the hypothalamic-pituitary-thyroid axis in zebrafish larvae. *Chemosphere* **87,** 1301–1307
18. Bouzaffour, M., Rampon, C., Ramaugé, M., Courtin, F., and Vriz, S. (2010) Implication of type 3 deiodinase induction in zebrafish fin regeneration. *Gen. Comp. Endocrinol.* **168,** 88–94
19. Popovic, M., Zaja, R., and Smital, T. (2010) Organic anion transporting polypeptides (OATP) in zebrafish (*Danio rerio*). Phylogenetic analysis and tissue distribution. *Comp. Biochem. Physiol. A Mol. Integr. Physiol.* **155,** 327–335
20. Walpita, C. N., Crawford, A. D., Janssens, E. D., Van der Geyten, S., and Darras, V. M. (2009) Type 2 iodothyronine deiodinase is essential for thyroid hormone-dependent embryonic development and pigmentation in zebrafish. *Endocrinology* **150,** 530–539
21. Walpita, C. N., Van der Geyten, S., Rurangwa, E., and Darras, V. M. (2007) The effect of 3,5,3′-triiodothyronine supplementation on zebrafish (*Danio rerio*) embryonic development and expression of iodothyronine deiodinases and thyroid hormone receptors. *Gen. Comp. Endocrinol.* **152,** 206–214
22. Arjona, F. J., de Vrieze, E., Visser, T. J., Flik, G., and Klaren, P. H. (2011) Identification and functional characterization of zebrafish solute carrier Slc16a2 (Mct8) as a thyroid hormone membrane transporter. *Endocrinology* **152,** 5065–5073
23. Elbaz, I., Yelin-Bekerman, L., Nicenboim, J., Vatine, G., and Appelbaum, L. (2012) Genetic ablation of hypocretin neurons alters behavioral state transitions in zebrafish. *J. Neurosci.* **32,** 12961–12972
24. Weinberg, E. S., Allende, M. L., Kelly, C. S., Abdelhamid, A., Murakami, T., Andermann, P., Doerre, O. G., Grunwald, D. J., and Riggleman, B. (1996) Developmental regulation of zebrafish MyoD in wild-type, no tail and spadetail embryos. *Development* **122,** 271–280
25. Urasaki, A., Morvan, G., and Kawakami, K. (2006) Functional dissection of the Tol2 transposable element identified the minimal cis-sequence and a highly repetitive sequence in the subterminal region essential for transposition. *Genetics* **174,** 639–649
26. Kawakami, K., Takeda, H., Kawakami, N., Kobayashi, M., Matsuda, N., and Mishina, M. (2004) A transposon-mediated gene trap approach identifies

developmentally regulated genes in zebrafish. *Dev. Cell* **7,** 133–144

27. Appelbaum, L., Skariah, G., Mourrain, P., and Mignot, E. (2007) Comparative expression of p2x receptors and ecto-nucleoside triphosphate diphosphohydrolase 3 in hypocretin and sensory neurons in zebrafish. *Brain Res.* **1174,** 66–75

28. Ben-Moshe, Z., Vatine, G., Alon, S., Tovin, A., Mracek, P., Foulkes, N. S., and Gothilf, Y. (2010) Multiple PAR and E4BP4 bZIP transcription factors in zebrafish. Diverse spatial and temporal expression patterns. *Chronobiol. Int.* **27,** 1509–1531

29. Lister, J. A., Robertson, C. P., Lepage, T., Johnson, S. L., and Raible, D. W. (1999) nacre encodes a zebrafish microphthalmia-related protein that regulates neural-crest-derived pigment cell fate. *Development* **126,** 3757–3767

30. Yaniv, K., Isogai, S., Castranova, D., Dye, L., Hitomi, J., and Weinstein, B. M. (2006) Live imaging of lymphatic development in the zebrafish. *Nat. Med.* **12,** 711–716

31. Kinne, A., Kleinau, G., Hoefig, C. S., Grüters, A., Köhrle, J., Krause, G., and Schweizer, U. (2010) Essential molecular determinants for thyroid hormone transport and first structural implications for monocarboxylate transporter 8. *J. Biol. Chem.* **285,** 28054–28063

32. Kinne, A., Schülein, R., and Krause, G. (2011) Primary and secondary thyroid hormone transporters. *Thyroid Res.* **4,** S7

33. García-Lecea, M., Kondrychyn, I., Fong, S. H., Ye, Z. R., and Korzh, V. (2008) *In vivo* analysis of choroid plexus morphogenesis in zebrafish. *PLoS One* **3,** e3090

34. Kim, C. H., Ueshima, E., Muraoka, O., Tanaka, H., Yeo, S. Y., Huh, T. L., and Miki, N. (1996) Zebrafish elav/HuC homologue as a very early neuronal marker. *Neurosci. Lett.* **216,** 109–112

35. Bernardos, R. L., and Raymond, P. A. (2006) GFAP transgenic zebrafish. *Gene Expr. Patterns* **6,** 1007–1013

36. Dutton, K., Abbas, L., Spencer, J., Brannon, C., Mowbray, C., Nikaido, M., Kelsh, R. N., and Whitfield, T. T. (2009) A zebrafish model for Waardenburg syndrome type IV reveals diverse roles for Sox10 in the otic vesicle. *Dis. Models Mech.* **2,** 68–83

37. Takada, N., and Appel, B. (2010) Identification of genes expressed by zebrafish oligodendrocytes using a differential microarray screen. *Dev. Dyn.* **239,** 2041–2047

38. Ji, C., Jin, X., He, J., and Yin, Z. (2012) Use of TSHβ:EGFP transgenic zebrafish as a rapid *in vivo* model for assessing thyroid-disrupting chemicals. *Toxicol Appl Pharmacol* **262,** 149–155

39. Darras, V. M., and Van Herck, S. L. (2012) Iodothyronine deiodinase structure and function. From ascidians to humans. *J. Endocrinol.* **215,** 189–206

40. Tatsumi, K., Hayashizaki, Y., Hiraoka, Y., Miyai, K., and Matsubara, K. (1988) The structure of the human thyrotropin β-subunit gene. *Gene* **73,** 489–497

41. Bernal, J., and Nunez, J. (1995) Thyroid hormones and brain development. *Eur. J. Endocrinol.* **133,** 390–398

42. Geysens, S., Ferran, J. L., Van Herck, S. L., Tylzanowski, P., Puelles, L., and Darras, V. M. (2012) Dynamic mRNA distribution pattern of thyroid hormone transporters and deiodinases during early embryonic chicken brain development. *Neuroscience* **221,** 69–85

43. Heuer, H., Maier, M. K., Iden, S., Mittag, J., Friesema, E. C., Visser, T. J., and Bauer, K. (2005) The monocarboxylate transporter 8 linked to human psychomotor retardation is highly expressed in thyroid hormone-sensitive neuron populations. *Endocrinology* **146,** 1701–1706

44. Nishimura, M., and Naito, S. (2008) Tissue-specific mRNA expression profiles of human solute carrier transporter superfamilies. *Drug Metab. Pharmacokinet.* **23,** 22–44

45. Sugiyama, D., Kusuhara, H., Taniguchi, H., Ishikawa, S., Nozaki, Y., Aburatani, H., and Sugiyama, Y. (2003) Functional characterization of rat brain-specific organic anion transporter (Oatp14) at the blood-brain barrier. High affinity transporter for thyroxine. *J. Biol. Chem.* **278,** 43489–43495

46. Ramadan, T., Camargo, S. M., Summa, V., Hunziker, P., Chesnov, S., Pos, K. M., and Verrey, F. (2006) Basolateral aromatic amino acid transporter TAT1 (Slc16a10) functions as an efflux pathway. *J. Cell. Physiol.* **206,** 771–779

47. Abe, S., Namba, N., Abe, M., Fujiwara, M., Aikawa, T., Kogo, M., and Ozono, K. (2012) Monocarboxylate transporter 10 functions as a thyroid hormone transporter in chondrocytes. *Endocrinology* **153,** 4049–4058

48. Wondisford, F. E., Radovick, S., Moates, J. M., Usala, S. J., and Weintraub, B. D. (1988) Isolation and characterization of the human thyrotropin β-subunit gene. Differences in gene structure and promoter function from murine species. *J. Biol. Chem.* **263,** 12538–12542

49. Van Herck, S. L., Geysens, S., Delbaere, J., Tylzanowski, P., and Darras, V. M. (2012) Expression profile and thyroid hormone responsiveness of transporters and deiodinases in early embryonic chicken brain development. *Mol. Cell. Endocrinol.* **349,** 289–297

50. Braun, D., Kinne, A., Bräuer, A. U., Sapin, R., Klein, M. O., Köhrle, J., Wirth, E. K., and Schweizer, U. (2011) Developmental and cell type-specific expression of thyroid hormone transporters in the mouse brain and in primary brain cells. *Glia* **59,** 463–471

51. Tonduti, D., Vanderver, A., Berardinelli, A., Schmidt, J. L., Collins, C. D., Novara, F., Di Genni, A., Mita, A., Triulzi, F., Brunstrom-Hernandez, J. E., Zuffardi, O., Balottin, U., and Orcesi, S. (2012) MCT8 deficiency. Extrapyramidal symptoms and delayed myelination as prominent features. *J. Child Neurol.,* in press

52. Xie, J., Farage, E., Sugimoto, M., and Anand-Apte, B. (2010) A novel transgenic zebrafish model for blood-brain and blood-retinal barrier development. *BMC Dev. Biol.* **10,** 76

53. Roberts, L. M., Woodford, K., Zhou, M., Black, D. S., Haggerty, J. E., Tate, E. H., Grindstaff, K. K., Mengesha, W., Raman, C., and Zerangue, N. (2008) Expression of the thyroid hormone transporters monocarboxylate transporter-8 (SLC16A2) and organic ion transporter-14 (SLCO1C1) at the blood-brain barrier. *Endocrinology* **149,** 6251–6261

54. Visser, W. E., Swagemakers, S. M., Ozgur, Z., Schot, R., Verheijen, F. W., van Ijcken, W. F., van der Spek, P. J., and Visser, T. J. (2010) Transcriptional profiling of fibroblasts from patients with mutations in MCT8 and comparative analysis with the human brain transcriptome. *Hum. Mol. Genet.* **19,** 4189–4200

55. Kogai, T., Liu, Y. Y., Richter, L. L., Mody, K., Kagechika, H., and Brent, G. A. (2010) Retinoic acid induces expression of the thyroid hormone transporter, monocarboxylate transporter 8 (Mct8). *J. Biol. Chem.* **285,** 27279–27288

56. Khalili, K., Del Valle, L., Muralidharan, V., Gault, W. J., Darbinian, N., Otte, J., Meier, E., Johnson, E. M., Daniel, D. C., Kinoshita, Y., Amini, S., and Gordon, J. (2003) Puralpha is essential for postnatal brain development and developmentally coupled cellular proliferation as revealed by genetic inactivation in the mouse. *Mol. Cell. Biol.* **23,** 6857–6875

57. Tanaka, K., Shouguchi-Miyata, J., Miyamoto, N., and Ikeda, J. E. (2004) Novel nuclear shuttle proteins, HDBP1 and HDBP2, bind to neuronal cell-specific cis-regulatory element in the promoter for the human Huntington disease gene. *J. Biol. Chem.* **279,** 7275–7286

58. Chan, Y. C., Roy, S., Khanna, S., and Sen, C. K. (2012) Down-regulation of endothelial microRNA-200b supports cutaneous wound angiogenesis by desilencing GATA binding protein 2 and vascular endothelial growth factor receptor 2. *Arterioscler. Thromb. Vasc. Biol.* **32,** 1372–1382

59. Kaufman, C. K., White, R. M., and Zon, L. (2009) Chemical genetic screening in the zebrafish embryo. *Nat. Protoc* **4,** 1422–1432

60. Kokel, D., Bryan, J., Laggner, C., White, R., Cheung, C. Y., Mateus, R., Healey, D., Kim, S., Werdich, A. A., Haggarty, S. J., Macrae, C. A., Shoichet, B., and Peterson, R. T. (2010) Rapid behavior-based identification of neuroactive small molecules in the zebrafish. *Nat. Chem. Biol.* **6,** 231–237